# Vibration Based Delamination Detection in Fiber Metal Laminates Composite Beam

**Omkar JARALI**
*Department of Mechanical Engineering, Vel Tech Rangarajan Dr. Sagunthala R&D Institute of Science and Technology, India,omkarjarali@gmail.com*

**Kamaraj LOGESH**
*Department of Mechanical Engineering, Vel Tech Rangarajan Dr. Sagunthala R&D Institute of Science and Technology, India,klogesh7@gmail.com*

**Vikas KHALKAR**
*Department of Mechanical Engineering, Gharda Institute of Technology, Lavel, India, vikas_khalkar@rediffmail.com*

**Pon HARIHARASAKTHISUDHAN**
*Department of Mechanical Engineering, Sri Krishna College of Technology, Kovaipudur, India, harimeed2012@gmail.com*

*Abstract:* - Delamination is typical damage in the Fiber Metal Laminate composite structures, usually hidden from the outer side that can reduce the structural stiffness. The delamination is undoubtedly an important topic as it causes to worsen the performance of the Fiber metal laminates (FMLs)structures in the service. The detection and severity analysis of delamination in a field like the aviation industry is vital for safety and economic considerations. The existence of delamination varies the vibration characteristics, such as natural frequencies, mode shapes, etc., of composites. Hence, this indication can be effectively used to locate and quantify the delamination. The changes in vibration characteristics are inputs for the inverse problem to determine the location and size of delamination. This paper used a machine-learning and regression model to determine the locations and severity of the delamination in the Fiber Metal laminate cantilever beams. The dataset related to delamination location, severity, and bending natural frequencies was obtained using the Finite Element Analysis. From this study, it is found that, the machine learning and regression model results related to predictions of delamination locations and severity are close to each other and give good agreement with actual delamination locations and delamination areas.

*Keywords:* - Natural frequency, Delamination, ANN, Regression, MATLAB, and ANSYS.

## 1. INTRODUCTION

The use of composite material in aerospace, naval, civil, and automobile industries is increasing due to its unique characteristics such as high strength-to-weight ratio, high specific strength, fatigue strength, and higher damage tolerance capability. Drilling operations [1, 2] on composite laminates Fiber metal laminates, Carbon fiber reinforced polymers (CFRPs), Glass fiber reinforced polymers (GFRPs) are necessary for fastening with different materials to have valued outcomes. Always, the quality of drilling determines the efficiency of fastening. It is expected to make error-free, precise holes in order to obtain high joint strength while assembling materials using riveting. However, the characteristics of the materials that make up composite laminates provide challenges during machining. Numerous unfavourable effects, i.e., pulling of fibers, delaminations, produces because of drilling operations. And it leads to reduce the materials fatigue strength. Figure 1 depicts the delamination of composite materials brought on by drilling operations. There is a significant difference between the drilling of conventional materials and composite materials. Drilling composite laminates is known to cause serious damage to the laminates, known as delamination. Delamination in the composite materials occurs during drilling operations because, during that time, thrust force and torque are produced and act on the materials. And it is considered one of the major modes of failure. The strength and stiffness of the composites are decreased by delamination. The dynamic response, or natural frequencies, changes as a result of the composites' altered stiffness. FMLs were the subject of a vibration investigation by Merzuki et al [3] (fiber metal laminates). They discovered through their research that natural frequencies rise along with lamina thickness. In fiber-metal laminates [4–9], alternative layers such as metal alloys and fiber-reinforced polymer composites are included. An aluminium alloy layer gives high impact strength to the composite materials. The relationship between delamination and the stacking sequence for composite materials is clearly explained by Long et al [10] Along with discussing how well delamination modelling works, they validated the damage model.

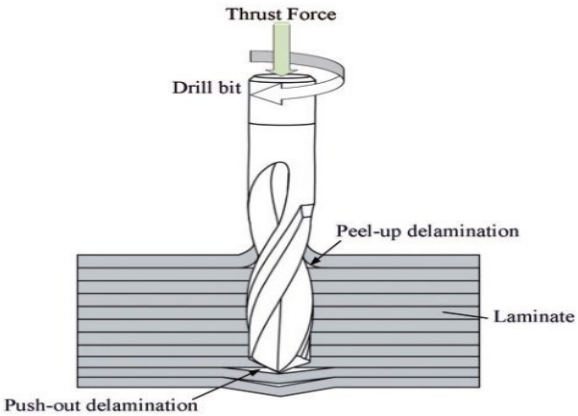


**Figure 1.** Delamination of composite material

To examine how delamination influences the eigen values (fundamental frequencies) and eigen vectors (mode shapes) of the dynamic response, Kim et al [11] developed a method for dynamic analysis. The derived model's generated natural frequencies, however, show strong agreement with both higher-order theoretical predictions and experimental results. Huang et al [12] investigated the GLARE-related characteristics of delamination extension and fatigue crack propagation under single overloads. To assess the behaviour of fatigue crack propagation and delamination extension, the applied loading variables were examined. The delamination resistance of laminated glass was tested by Dural and Oyar [13] under varied boundary conditions.

De-Vries et al [14] conducted an experimental programme to evaluate different splicing geometry and the thicknesses of the metal layer for delamination behaviour. Given the scatter in the results discussed in this article, it is imperative to design the yield function using an appropriate test approach first. The squared weighted deviation between the observed mode form of a composite plate with delamination and it is used to create a weighted eigen vector damage index [15]. It is investigated whether delamination can be detected using a vibration test in addition to the effects of the area of delamination on the plate's inherent frequencies [16]. The laminated (orthotropic) composite plate's theoretical natural frequency is determined using the D'Alembert concept. The intrinsic frequencies of the plate are significantly impacted by lamination delamination in composite laminates [17]. Delamination tests were conducted, and the results were compared with predictions of linear damage growth. The delaminated surfaces were examined by scanning electronic microscopy to more fully evaluate the delamination growth rate under different amplitude loadings.

Khan et al [18] investigated how variations in stress influenced the pattern of delamination in fiber-metal laminates. The creation of delamination shapes under varying amplitude loading is described with an explanation. The transient behaviour of a delaminated composite plate with integrated active fiber composite was studied by Shankar et al [19]. By carefully examining the digital imagecorrelation (DIC) results [20], it was possible to evaluate how various delamination behaviours during testing affected the compressive load capacity. The presence of delaminations in the composite structures introduces a local flexibility in the damage location, which changes the dynamic behavior of the composite, because of reduction in the stiffness. Thus, vibration analysis can be the best tool for delaminations assessment, as the reduction in the stiffness results in changes in the natural frequencies and modifications of the mode shapes, impulsive response, frequency response functions, etc. of the component [21, 22] while the existence of damage can be easily identified by monitoring natural frequency shifts, identifying the location and severity of this damage is not possible directly. It can be done by solving the inverse problem, which requires the use of artificial intelligence [23, 24]. Vibration-based composite health monitoring through monitoring dynamic response of composite structures is the research work carried out and reported here. Fiber metal laminate (FMLs) composite beams were chosen for this study. Composite structures in their lifetime can suffer from a number of failure mechanisms like delaminations, fiber breakage, matrix cracking, etc, due to impacts of foreign objects, fatigue loads, environmental conditions, etc. Delamination in composite structures may easily spread throughout the composite laminate upon repeated loading, causing disastrous and costly failures. Srikant et al [27] considered and used the differences in the vibrational characteristics as inputs to predict the delamination location and size. This study uses an artificial neural network with the natural frequency as the standard vibration parameter to examine the delamination of a glass fiber-reinforced composite beam. (ANN). The results demonstrate that the back propagation method based on artificial neural networks can perfectly predict the quantity and position of delaminations in composites, given numerical natural frequency data. Zhang et al

[28] expanded the graphical method to estimate the delamination variables in anisotropic composite beams. After the'Introduction' section, the organization of the research paper is presented using the flowchart. The flow chart is shown in Figure 2.

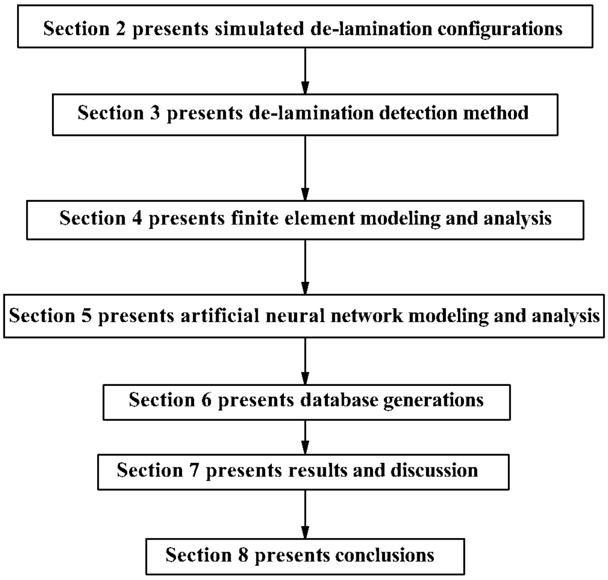


**Figure 2.** A flowchart shows the organization of the research paper after the introduction section

## 1.1. The novelty of the present work

The authors have reviewed plenty of research papers on delamination of composite beams and plates, i.e., Liu et al. [1], Shankar et al. [2], Sultan et al. [22], Srikanth et al. [27], and Zhang et al. [28], on glass fiber reinforced polymers beams, carbon fiber reinforced polymers beams, woven fiber glass laminate plates, epoxy composite laminate plates, etc. They found very limited papers on vibration studies of delaminated fiber metal laminate beams. This motivated the authors to do the delamination detection in fiber metal laminate composite beams because of their practical importance, and this is the main novelty of this research study.

In this research study, for better estimation of severity (size) and location of the delamination, the problem is divided into two phases. The first phase is training the natural frequencies for different delamination scenarios and is generated using artificial neural networks, for which a dataset of the first five natural frequencies for different delamination scenarios is generated using finite element modeling techniques. Similarly, a regression model was developed using the dataset of first normalized natural frequency and the normalized delamination location. In the regression model, the natural frequency and the delamination location act as a dependent and independent variable. Equation 5 gives the relationship between the normalized natural frequency and normalized delamination location. During the second phase, the inverse problem is solved using artificial neural networks and regression models to predict the delamination parameters.

## 1.2. Material and geometric properties of the beam

The material properties and geometric properties of the FML (Aluminum, Glass fibers, and Carbon fibers) were taken from the previous study [3]. The material properties are presented in the Table 1 and Table 2.

**Table 1.** Material properties of Aluminum sheet [3]

| Property | Aluminum |
|---|---|
| $E_1$ $(N/m^2)$ | 70.6 |
| Þ $(kg/m^3)$ | 2780 |
| $\mu$ | 0.3 |

**Table 2**. Material properties of FMLs composite beam [3]

| Property | Glass fiber epoxy | Carbon fiber epoxy |
|---|---|---|
| $E_1$ $(N/m^2)$ | 7e9 | 17.5e9 |
| $E_2$ $(N/m^2)$ | 1e9 | 5e9 |
| $E_3$ $(N/m^2)$ | 7e9 | 17.5e9 |
| $G_{12}$ $(N/m^2)$ | 2.5e9 | 10.5e9 |
| $G_{13}$ $(N/m^2)$ | 1e9 | 2e9 |
| $G_{23}$ $(N/m^2)$ | 2.5e9 | 10.5e9 |
| $\mu_{12}$ | 0.22 | 0.24 |
| $\mu_{13}$ | 0.22 | 0.24 |
| $\mu_{23}$ | 0.22 | 0.24 |
| $\rho$ $(kg/m^3)$ | 2440 | 1750 |

In order to do the de-lamination study in the present research paper, a 2/1 configuration of FML composite beam (Aluminum/Glass fiber epoxy/Aluminum) was considered. In this study, the material properties presented in Table 1 and Table 2 were considered. The new geometric properties were chosen in the present research study and they are presented in Table 3.

**Table 3**. Geometric properties of FML composite beam

| Materials | Length (mm) | Width (mm) | Thickness (mm) |
|---|---|---|---|
| Al | 500 | 25 | 0.88 |
| GF-E | 500 | 25 | 2.56 |

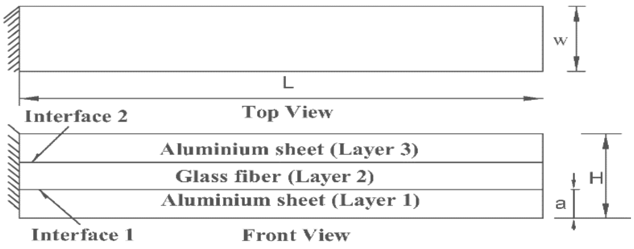


**Figure 3.** Intact FML (AL/GF-E/AL) 2/1 configurations composite beam

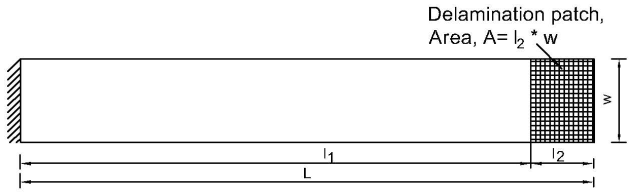


**Figure 4.** Delaminated FML (AL/GF-E/AL) 2/1 configurations composite beam

## 2. SIMULATED DE-LAMINATION CONFIGURATIONS

In this research study, eighty-seven specimens were considered. This study was further divided into case 1 and case 2. In case 1, one intact specimen was considered to normalize the first five bending natural frequencies. In case 2, 86 specimens were there, and all these specimens carried the delamination patch along the entire width. The one case of intact (non-delaminated) composite beam and delaminated composite beam is shown in Figure3 and Figure4, respectively. This case was again divided into two sub-cases, i.e., sub-case 1 and sub-case 2.

**Sub-case 1:** This sub-case carried 43 specimens. De-lamination was provided between the first and second layers, and perfect bonding was there between the second and third layers. The delamination length on the specimens was varied from 5 mm to 215 mm by an interval of 5 mm from the free end of the composite beam.

**Sub-case 2:** This sub-case was like sub-case 1; the only difference was that instead of layer number 1 and layer number 2, the delamination was considered between layer number 2 and layer number 3. It is also shown in Figure 2.

## 3. DELAMINATION DETECTION METHOD

### 3.1. Inverse method of delamination detection using a regression model

This research study proposes a regression model as a forward approach between the normalized natural frequency and normalized delamination location. It is given in Equation (1).

$$\boldsymbol{Y = f\left(\frac{l_1}{L}\right)} \quad (1)$$

$Y$ is the ratio between the natural frequency of the delaminated beam and the natural frequency of the intact composite beam.
$l_1/L$ is the ratio of the distance of the delamination from the cantilevered end to the length of the beam.

$$\boldsymbol{Y - f\left(\frac{l_1}{L}\right) = 0} \quad (2)$$

Then, an inverse method using a regression model is proposed to predict the delamination location in the cantilever beam. The regression model was developed using the dataset presented in the Table 5. Only one dependent variable ($\mathbf{f_{r1}}$) and one independent variable ($l_1/L$) was considered to develop the regression model. The Equation (4) was used to predict the delamination location ratio ($l_1/L$). To determine the delamination locations in a cantilever beam, the first normalized natural frequency ($f_{r1}$) was used and, it was substituted in Equation (5). Afterward, Equation (4) was used to compute the delaminated area. $l_2$ and $w$ are the length and width of the delamination, respectively, are shown in Figure 4. Delamination was considered along the entire width of the beam. The delamination patch $(A = w * l_2)$on the composite beam is also shown in Figure 4.

$$\boldsymbol{l_1 + l_2 = L}$$

$$\boldsymbol{l_2 = L - l_1} \quad (3)$$

$$\boldsymbol{A = w * l_2} \quad (4)$$

### 3.2. Correlation model

The natural frequency of the delaminated beam was normalized with that of the intact beam. $Y$ is the normalized natural frequency in the first bending mode. The normalized natural frequency($\boldsymbol{Y}$) was plotted against the delamination location ratio$\left(\frac{l_1}{L}\right)$. The first bending natural frequency was used to obtain the regression model for the curve fitting. Only one Equation was required to find an unknown parameter, i.e., delamination location. Based on the non-linear relationship between the delamination parameter and frequency ratios, non-linear polynomial curve fitting was used to get the first natural frequency ratio equation at the first mode. Equation 5 was developed using the data set of delaminated composite beam specimens. The second-order correlation model presented in Equation (5) was generated by regression analysis using Microsoft Excel. The R-squared values generally determine the reliability of the correlation models. The R-squared value nearer to '1' represents the excellent fit of the data on the generated correlation models. In the present work, the R-squared values of the generated correlation models are shown in Figure 5. To determine the delamination locations in a cantilever beam, the first normalized natural frequency was used and, it was substituted in Equation (5). Delamination location ratios computed using the Microsoft Excel solver. In this research study, FMLs composite beam was analyzed for the first five natural bending frequencies. To develop the regression model, first natural frequencies were considered.

$$-0.0011\left(\frac{l_1}{L}\right)^2 + 0.003\left(\frac{l_1}{L}\right) + 0.9981 = Y$$

$$-0.0011\left(\frac{l_1}{L}\right)^2 + 0.003\left(\frac{l_1}{L}\right) + 0.9981 - Y = 0 \quad (5)$$

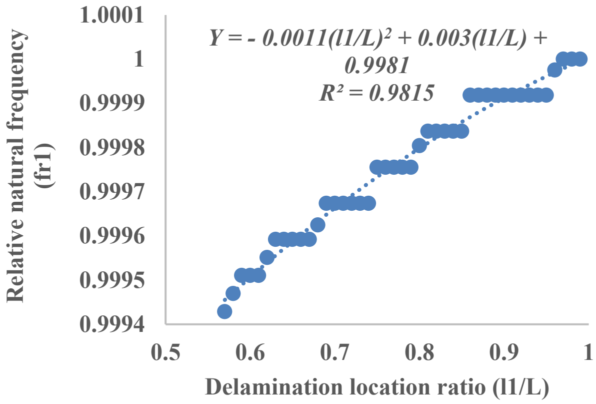


**Figure 5.** Regression model between first relative bending natural frequency ($f_1/fn_1$) and delamination location ratio ($l_1/L$).

## 4. FEA MODELING AND ANALYSIS

ANSYS 12.1 commercial software was the FE tool used to create a finite element model of undamaged and delaminated three-dimensional cantilever composite beams. The beam model used here was made up of a 3-layer laminate. The material property of the composite beam (for giving input in FEA) was obtained through previous studies. Furthermore, all these properties are given in Table 1 and Table 2. The solid 185 layered element was used for modeling the beams as the composite beam is under the three-dimensional modeling of solid structures. Shell elements define information regarding each layer. A shell element was used to give the information about each layer. Moreover, only one element was considered along the thickness of each layer. A mesh sensitivity analysis was performed, and the optimum number of elements was determined to achieve the balance between the computational time and model parameter accuracy. Contact elements (CONTAC173) and target elements (TARGET 170) ensure the perfect bonding and de-bonding between the two surfaces. The first five bending natural frequencies of the delaminated beams were obtained using the modal analysis ANSYS. The first five bending natural frequencies of delaminated FML composite beams are presented in Table 5. Similarly, the first three bending natural frequencies, non-delaminated FML composite beam [3], are presented in Table 6.

## 5. ARTIFICIAL NEURAL NETWORK MODELING AND ANALYSIS

ANN technique is used for delamination prediction in beams. The ability to learn from experience in order to enhance results is the most important aspect of ANN. As a consequence, ANN can be used in a number of applications, including classification, control systems, detection, image processing, and pattern recognition. The artificial Neural Network classifier is based on the human brain structure. Nodes are connected with the neurons in the brain. It is a feed-forward artificial neural network where the mapping between inputs and output is nonlinear. It has input and output layers and multiple hidden layers with many neurons [25, 26]. The learning methodology adopted to train an ANN is Back propagation. The learning process combines many hidden layers, the number of nodes in each of the hidden layers, and connection weight. Backpropagation allows for the adjustment of the weights in the network iteratively. Inputs were combined with the initial weights and fed to the nonlinear activation function. From the hidden layers to the output layer, each layer's output is fed as input to the next layer. Output is compared with the expected value. The computed errors are propagated backward from the output to the preceding layer. The error propagated back to adjusting the interconnection weights between the layers. Back propagation is done using a Gradient Descent. The partial derivative of the Mean Squared Error function was calculated for interconnection weights. Then, to propagate the error back, the weights of the first hidden layer were updated with the gradient value. This process kept going until the gradient for each input-output pair converged. The hyper parameters of the neural network are presented in Table 4.

The information regarding input, hidden layer and output layer is shown in Figure 6. The ANN model was implemented with three input layers, ten hidden layers, and two output layers. First, five normalized bending natural frequencies presented in Table 5 were chosen as input parameters; relative delamination location was selected as the output parameter. ANN maps these inputs with the output. Using the hyper-parameters, the ANN model was tuned.

The hyper-parameters are listed in Table 4. Artificial neural networking (ANN) in MATLAB is used to analyse and predict the location of delamination in the beam. In MATLAB, the desired inputs and output or target are imported into the workspace and, using the "nntool" network, is created using inputs and targets. Here, a typical three-layered Feed Forward Back Propagation (FFBP) neural network is considered.The first five normalized natural frequencies ($fr_1$, $fr_2$, $fr_3$, $fr_4$and $fr_5$) were taken as input parameters; delamination location was taken as the output parameter($l_1/L$, $A$).

The various functions used are: Levenberg Marquardt (trainlm) is taken as a training function, LEARNGDM is taken as an adaption learning function, mean square error (MSE) taken as a performance function and Sigmoid function (tansig) as a transfer function.

The regression plot regarding training, validation and testing is shown in Figure 7. It shows that the predicted data is well fitted to the actual output.

**Table 4.** Hyper-parameter of Artificial Neural Network

| Sr. No. | Input parameters for training | Values |
|---|---|---|
| 01 | Learning rate | 0.1 |
| 02 | Number of epochs | 1000 |
| 03 | Number of nodes in input layer | 05 |
| 04 | Number of neurons in the hidden layer | 10 |
| 06 | Number of nodes in output layer | 01 |
| 07 | Goal | zero |

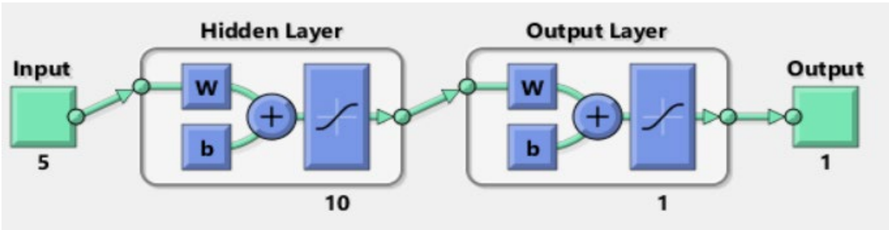


**Figure 6.** Feed forward back propagation neural network

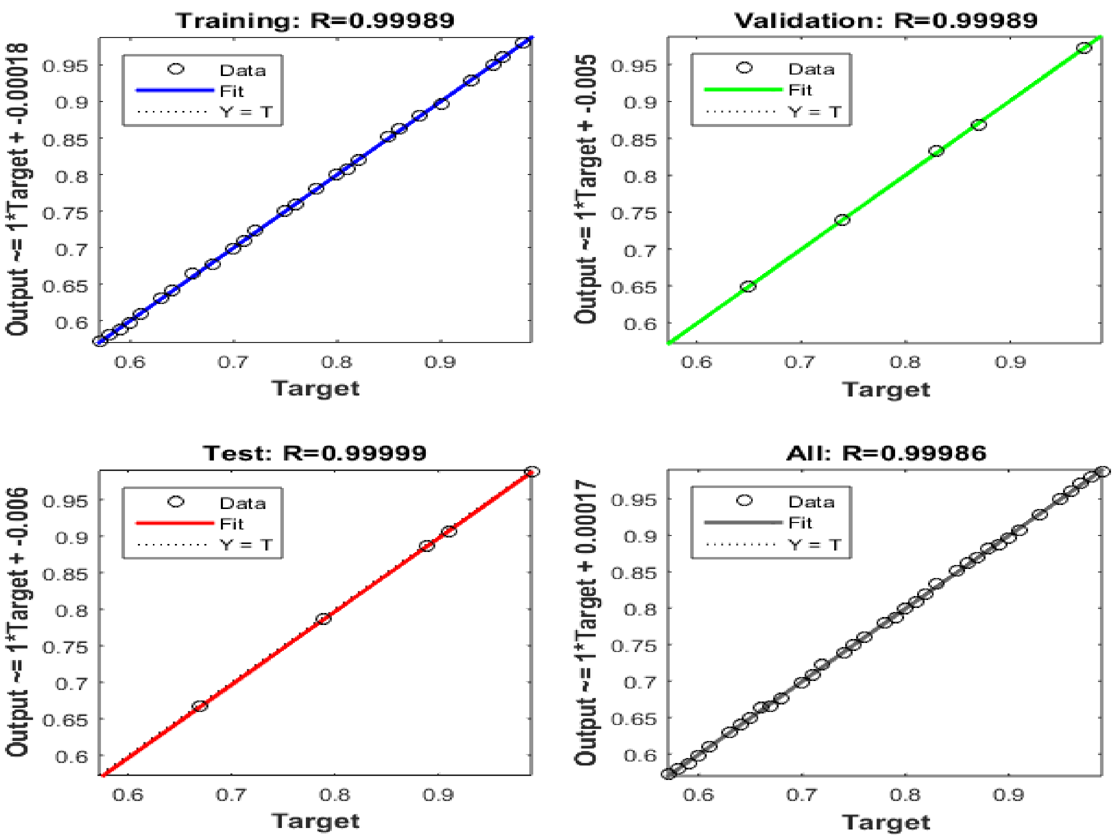


**Figure 7.** Regression plot

**Table 5.** Training data of normalized natural frequencies (interface 1) to the neural network

| *Sr. No.* | *$L_1/L$* | *$fr_1$* | *$fr_2$* | *$fr_3$* | *$fr_4$* | *$fr_5$* |
|---|---|---|---|---|---|---|
| **Interface 1** | | | | | | |
| **01** | 0.99 | 1 | 1 | 1 | 0.999955157 | 0.999969568 |
| **02** | 0.98 | 1 | 0.999984415 | 1 | 0.999910314 | 0.999957395 |
| **03** | 0.97 | 1 | 0.999965367 | 1 | 0.999865471 | 0.999939136 |
| **04** | 0.96 | 0.999975518 | 0.999954978 | 1 | 0.999641256 | 0.999920876 |
| **05** | 0.95 | 0.999918394 | 0.999948051 | 1 | 0.999820628 | 0.999878271 |
| **06** | 0.94 | 0.999918394 | 0.999941125 | 1 | 0.999798206 | 0.999872794 |
| **07** | 0.93 | 0.999918394 | 0.999930735 | 1 | 0.999775785 | 0.999872185 |
| **08** | 0.92 | 0.999918394 | 0.999930735 | 1 | 0.999775785 | 0.999869142 |
| **09** | 0.91 | 0.999918394 | 0.999930735 | 1 | 0.999775785 | 0.999866099 |
| **10** | 0.9 | 0.999918394 | 0.999923808 | 1 | 0.9997713 | 0.999864881 |
| **11** | 0.89 | 0.999918394 | 0.999913418 | 1 | 0.9997713 | 0.999863055 |
| **12** | 0.88 | 0.999918394 | 0.999906492 | 0.999993974 | 0.999772646 | 0.999861838 |
| **13** | 0.87 | 0.999918394 | 0.999896102 | 0.999992467 | 0.9997713 | 0.999860012 |
| **14** | 0.86 | 0.999918394 | 0.999896102 | 0.999990207 | 0.9997713 | 0.999858795 |
| **15** | 0.85 | 0.999836788 | 0.999896102 | 0.999984934 | 0.9997713 | 0.999856969 |
| **16** | 0.84 | 0.999836788 | 0.999882249 | 0.999981921 | 0.999769058 | 0.999855752 |
| **17** | 0.83 | 0.999836788 | 0.999878786 | 0.999977401 | 0.999766816 | 0.999853926 |
| **18** | 0.82 | 0.999836788 | 0.999878786 | 0.999962335 | 0.999764126 | 0.999850883 |
| **19** | 0.81 | 0.999836788 | 0.999878786 | 0.999932203 | 0.999762332 | 0.999847839 |
| **20** | 0.8 | 0.999804146 | 0.999878786 | 0.999917137 | 0.999758296 | 0.999844796 |
| **21** | 0.79 | 0.999755182 | 0.999878786 | 0.999887006 | 0.999753363 | 0.99983871 |
| **22** | 0.78 | 0.999755182 | 0.999878786 | 0.999849341 | 0.999749327 | 0.999835666 |
| **23** | 0.77 | 0.999755182 | 0.999878786 | 0.999811676 | 0.999744395 | 0.99982958 |
| **24** | 0.76 | 0.999755182 | 0.999878786 | 0.999736347 | 0.999735426 | 0.999823494 |
| **25** | 0.75 | 0.999755182 | 0.999878786 | 0.999706215 | 0.999730942 | 0.999817407 |
| **26** | 0.74 | 0.999673576 | 0.999878786 | 0.999608286 | 0.999726457 | 0.999814364 |
| **27** | 0.73 | 0.999673576 | 0.999878786 | 0.999570621 | 0.999721973 | 0.999805234 |
| **28** | 0.72 | 0.999673576 | 0.999878786 | 0.999472693 | 0.999717489 | 0.999802191 |
| **29** | 0.71 | 0.999673576 | 0.999878786 | 0.999382298 | 0.99970852 | 0.999796105 |
| **30** | 0.7 | 0.999673576 | 0.999864933 | 0.99926177 | 0.999704036 | 0.999790018 |
| **31** | 0.69 | 0.999673576 | 0.999861469 | 0.999156309 | 0.999699552 | 0.999786975 |
| **32** | 0.68 | 0.999624612 | 0.999861469 | 0.99900565 | 0.999695067 | 0.999783932 |
| **33** | 0.67 | 0.99959197 | 0.999861469 | 0.998877589 | 0.999690583 | 0.999780889 |
| **34** | 0.66 | 0.99959197 | 0.999854543 | 0.998870056 | 0.999688789 | 0.999779671 |
| **35** | 0.65 | 0.99959197 | 0.999844153 | 0.998561205 | 0.999686099 | 0.999777845 |
| **36** | 0.64 | 0.99959197 | 0.999835495 | 0.998403013 | 0.999683857 | 0.999776019 |
| **37** | 0.63 | 0.99959197 | 0.999826837 | 0.998207156 | 0.999681614 | 0.999774802 |
| **38** | 0.62 | 0.999551167 | 0.99981991 | 0.997973635 | 0.999681614 | 0.999774802 |
| **39** | 0.61 | 0.999510364 | 0.999809521 | 0.997845574 | 0.999681614 | 0.999774802 |
| **40** | 0.6 | 0.999510364 | 0.999792204 | 0.997649718 | 0.999681614 | 0.999774802 |
| **41** | 0.59 | 0.999510364 | 0.999774888 | 0.99747646 | 0.999681614 | 0.999774802 |
| **42** | 0.58 | 0.999469561 | 0.993004208 | 0.997288136 | 0.999681614 | 0.999774802 |
| **43** | 0.57 | 0.999428758 | 0.999722939 | 0.997129944 | 0.999681614 | 0.999774802 |

## 6. DATABASE GENERATION

For training the inverse algorithm, a database consisting of shifts in natural frequencies is required because of known delaminations. As analytical expressions for vibration of the delaminated composites are complicated and conducting experiments is costly, the required database is generated with the help of a finite element tool. FE simulation was conducted on many composite beam models with different sizes and locations of delamination. The database size used for training ANN plays a crucial role in accurately determining the delamination's (location and severity). For this work, 43 different delamination scenarios were generated numerically. The first five natural frequencies were obtained for all the delamination scenarios and they were used as input to ANN while delamination location ratio and size were used as output to ANN. Thirty-seven input–output datasets were given to the ANN for training purposes and the rest were used for the validation process.

## 7. RESULTS AND DISCUSSION

In order to check the correctness of the approach to the numerical modeling, four cases of previously published papers were solved to get the first three bending natural frequencies.

The obtained numerical bending natural frequencies were compared with the published experimental results, and good agreement was found. The results of natural frequencies of all the configurationare presented in Table 6.

In this study, free vibrations of intact and later delaminated beams that had different delamination locations and areas were investigated numerically. The natural frequencies of the beams were determined and then the relationship between the delamination locations and the variation in the natural frequency was investigated.

The first five bending natural frequencies were determined for the intact and delaminated beams using the numerical method. Afterwards, the natural frequencies were normalized (natural frequency of delaminated beam and natural frequency of non-delaminated or intact beam). The data set of normalized natural frequencies was used to develop the regression model and machine learning model.

In order to detect the location and severity of delamination in a 2/1 (Aluminum/Glass fiber epoxy/Aluminum) configuration, FML composite beam was considered. The same material properties of the previous study were considered and used. It is presented in Table 1 and Table 2.

The delamination study's chosen geometric properties of composite beams are presented in Table 3. To develop the machine learning and regression model the dataset presented in Table 5 was referred. The predicted delamination locations and severity give a good agreement and theyare shown in Figure 8 and 9. It is also presented in the Table 7 to Table 10.

Figures 8and 9 show the predicted delamination locations and severity using the machine learning and regression models in composite beams. It was found that the ANN (Machine learning model) and regression model gave good results regarding the prediction of delamination locations and severity.

The machine learning model gave -0.3809% and 3.536% as the maximum error while predicting the delaminationlocations and areas. Furthermore, the regression model gave -4.71% and 30.95% as the maximum error to predict the delamination locations and area. Similarly, the Machine learning model gave 0.1449% and 0.3215 % as minimum error while predicting the delamination locations and delamination area. And the regression model gave -0.1904 % and -1.01% as a minimum errors while predicting the delamination locations and delamination area.

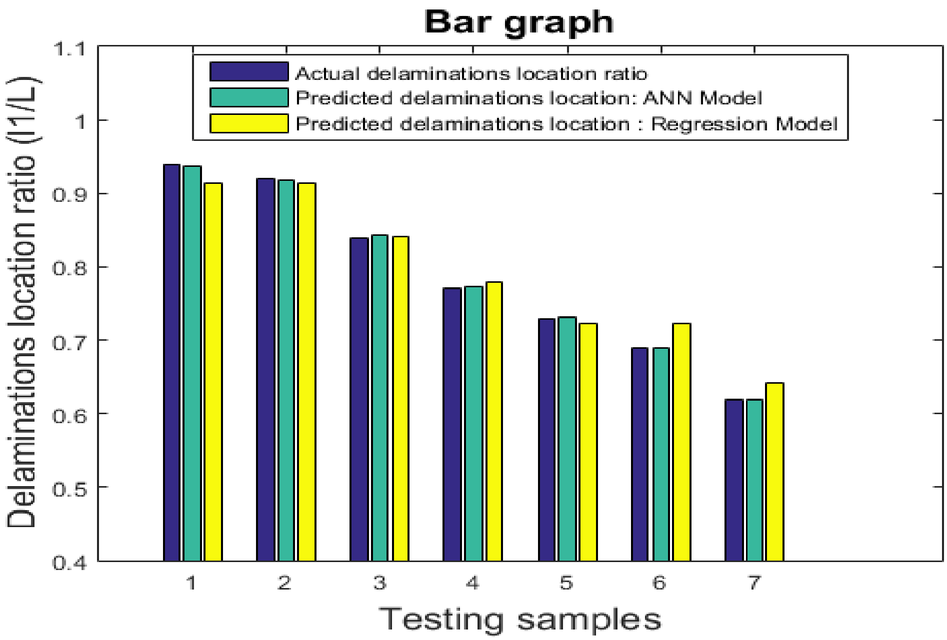


**Figure 8.** Predicted delamination ratio for different samples using machine learning and regression model

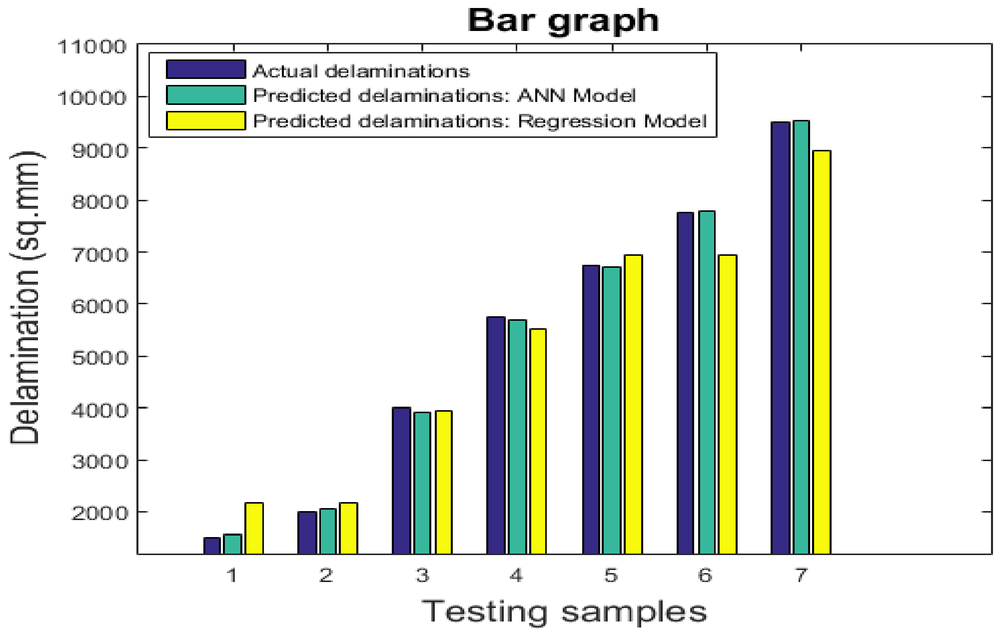


**Figure 9.** Predicted delamination area for different samples using the machine learning and regression model

**Table 6.** Numerical and experimental bending natural frequencies ($f_1$, $f_2$and $f_3$) of 2/1(H1 and H2) and 3/2 (H3 and H4)configurations of fiber metal laminate composite beam

| Configurations of FMLs beam | $f_1$ (hz) Exp. [3] | $f_1$ (hz) Numerical | % error | $f_2$ (hz) Exp. [3] | $f_2$ (hz) Numerical | % error | $f_3$ (hz) Exp. [3] | $f_3$ (hz) Numerical | % error |
|---|---|---|---|---|---|---|---|---|---|
| H1 (2/1) | 29.03 | 28.497 | 1.83 | 187 | 178.34 | 4.63 | 525 | 498.81 | 4.98 |
| H2 (2/1) | 21.5 | 28.29 | 24 | 159 | 177.06 | 10.19 | 458 | 495.28 | 7.52 |
| H3 (3/2) | 48.64 | 45.512 | 6.43 | 298 | 284.58 | 4.5 | 871 | 794.4 | 8.79 |
| H4 (3/2) | 41.77 | 40.203 | 3.75 | 266 | 251.66 | 5.39 | 716 | 704.431 | 1.61 |

**Table 7.** Comparison between Actual and predicted ANN outputs of delamination location.

| *fr1* | *fr2* | *fr3* | *fr4* | *fr5* | Actual, *L1/L* | Predicted, *L1/L* | % error |
|---|---|---|---|---|---|---|---|
| 0.99991839 | 0.99994112 | 1 | 0.99979820 | 0.99987279 | 0.94 | 0.9378 | 0.2340 |
| 0.9999183 | 0.99993073 | 1 | 0.999775785 | 0.999869142 | 0.92 | 0.9179 | 0.2282 |
| 0.99983678 | 0.99988224 | 0.9999819 | 0.999769058 | 0.999855752 | 0.84 | 0.8432 | -0.3809 |
| 0.99975518 | 0.99987878 | 0.9998116 | 0.999744395 | 0.99982958 | 0.77 | 0.7723 | -0.2987 |
| 0.99967357 | 0.99987878 | 0.9995706 | 0.999721973 | 0.999805234 | 0.73 | 0.7319 | -0.2602 |
| 0.99967357 | 0.99986146 | 0.9991563 | 0.999699552 | 0.999786975 | 0.69 | 0.689 | 0.1449 |
| 0.9995511 | 0.99981991 | 0.9979736 | 0.999681614 | 0.999774802 | 0.62 | 0.6186 | 0.2258 |

**Table 8.** Comparison between Actual and predicted ANN outputs of delamination area

| *fr1* | *fr2* | *fr3* | *fr4* | *fr5* | Actual,*A* | Predicted, *A* | % error |
|---|---|---|---|---|---|---|---|
| 0.99991839 | 0.99994112 | 1 | 0.99979820 | 0.99987279 | 1500 | 1555 | 3.536 |
| 0.9999183 | 0.99993073 | 1 | 0.999775785 | 0.999869142 | 2000 | 2052.5 | 2.557 |
| 0.99983678 | 0.99988224 | 0.9999819 | 0.999769058 | 0.999855752 | 4000 | 3920 | -2.04 |
| 0.99975518 | 0.99987878 | 0.9998116 | 0.999744395 | 0.99982958 | 5750 | 5692.5 | -1.01 |
| 0.99967357 | 0.99987878 | 0.9995706 | 0.999721973 | 0.999805234 | 6750 | 6702.5 | -0.708 |
| 0.99967357 | 0.99986146 | 0.9991563 | 0.999699552 | 0.999786975 | 7750 | 7775 | 0.3215 |
| 0.9995511 | 0.99981991 | 0.9979736 | 0.999681614 | 0.999774802 | 9500 | 9535 | 0.367 |

**Table 9.** Comparison between Actual and predicted regression model outputs of delamination location

| *fr1* | *fr2* | *fr3* | *fr4* | *fr5* | Actual, L1/L | Predicted, L1/L | % error |
|---|---|---|---|---|---|---|---|
| 0.99991839 | 0.99994112 | 1 | 0.99979820 | 0.99987279 | 0.94 | 0.9131 | 2.861 |
| 0.9999183 | 0.99993073 | 1 | 0.999775785 | 0.999869142 | 0.92 | 0.9131 | 0.75 |
| 0.99983678 | 0.99988224 | 0.9999819 | 0.999769058 | 0.999855752 | 0.84 | 0.8416 | -0.1904 |
| 0.99975518 | 0.99987878 | 0.9998116 | 0.999744395 | 0.99982958 | 0.77 | 0.7795 | -1.233 |
| 0.99967357 | 0.99987878 | 0.9995706 | 0.999721973 | 0.999805234 | 0.73 | 0.7225 | 1.027 |
| 0.99967357 | 0.99986146 | 0.9991563 | 0.999699552 | 0.999786975 | 0.69 | 0.7225 | -4.71 |
| 0.9995511 | 0.99981991 | 0.9979736 | 0.999681614 | 0.999774802 | 0.62 | 0.6423 | -3.596 |

**Table 10.** Comparison between Actual and predicted regression model outputs of delamination area

| *fr1* | *fr2* | *fr3* | *fr4* | *fr5* | Actual, A | Predicted, A | % error |
|---|---|---|---|---|---|---|---|
| 0.99991839 | 0.99994112 | 1 | 0.99979820 | 0.99987279 | 1500 | 2172.5 | 30.95 |
| 0.9999183 | 0.99993073 | 1 | 0.999775785 | 0.999869142 | 2000 | 2172.5 | 7.94 |
| 0.99983678 | 0.99988224 | 0.9999819 | 0.999769058 | 0.999855752 | 4000 | 3960 | -1.01 |
| 0.99975518 | 0.99987878 | 0.9998116 | 0.999744395 | 0.99982958 | 5750 | 5512.5 | -4.308 |
| 0.99967357 | 0.99987878 | 0.9995706 | 0.999721973 | 0.999805234 | 6750 | 6937.5 | 2.702 |
| 0.99967357 | 0.99986146 | 0.9991563 | 0.999699552 | 0.999786975 | 7750 | 6937.5 | -11.71 |
| 0.9995511 | 0.99981991 | 0.9979736 | 0.999681614 | 0.999774802 | 9500 | 8942.5 | -6.234 |

## 8. CONCLUSIONS

In this study, vibration-based analysis is used on FMLs composite beams to predict the delamination's location and severity. It was observed that delamination in composite beams significantly degrades natural frequencies. The first and third natural frequencies degrade significantly with increasing delamination size compared to the second, fourth, and fifth natural frequencies. First, five natural frequencies are input to ANN, and delamination scenarios (locations and sizes) are taken as output. A Dataset consisting of 43 input-output pairs has been generated from different delamination scenarios and used for the training and validation of a feed-forward multilayer back-propagation Artificial Neural Network. Numerically simulated frequency data evaluated the ANN and Regression model's location and severity prediction accuracy. The ANN and regression model predicts delamination length and area with better accuracy. Hence, a neural controller can be programmed, trained, and installed on the structure for structural health monitoring. Then it will lead to giving the damage information accurately.

## REFERENCES


[1] D Liu, Y Tang, W L Cong, A review of mechanical drilling of composite laminates, *Composite Structures,* Vol. 94, No. 4, 2012, pp. 1265 – 1279.

[2] B.R. Shankar, P. Umamaheswarrao , A.V. Avinash Reddy , P. Koushik Kumar, Drilling of composite laminates- A Review, *Journal of Basic and Applied Engineering Research,*Vol. 1, No. 3, 2014, pp. 19-24.

[3] M N M Merzuki, M R M Rejab, M S M Sani, B Zhang, M Quanjin. Experiemental investigation of free vibration analysis on fibre metal laminates, *Journal of Mechanical Engineering and Sciences,* Vol. 13, No. 4, 2019, pp. 5753 – 5763.

[4] Sinmazcelik T, Avcu E, Bora M O, Coban O, A review: Fibre metal laminates, background, bonding types and applied test methods, *Materials and Design,* Vol.32, 2011w, 3617- 3685.

[5] Iriondo J, Aretxabaleta L, Aizpuru A. Charecterization of the elastic and damping properties of FML and FML based on a self-reinforced polypropylene, *composite structures,* Vol. 131, 2015, pp. 47- 54.

[6] Rajkumar G, Krishna M, Narasimhamurthy H, Keshavamurthy Y, Nataraj J. Investigation of tensile and bending behavior of aluminum based hybrid fiber metal laminates. *Procedia Materials Science.*Vol. 5, 2014, pp. 60-68.

[7] Ahmadi H, Liaghat G, Sabouri H, Bidkhouri E. Investigation on the high velocity impact properties of glass-reinforced fiber metal laminates. *Journal of Composite Materials,* Vol. 47, 2013, pp. 1605-1615.

[8] Ghasemi AR, Mohandes M. Free vibration analysis of rotating fiber–metal laminate circular cylindrical shells. *Journal of Sandwich Structures and Materials,* Vol. 9, 2017, pp. 63- 72.

[9] Tooski MY, Alderliesten R, Ghajar R, Khalili S. Experimental investigation on distance effects in repeated low velocity impact on fiber–metal laminates. *Composite Structures.*Vol. 99, 2013, pp. 31-40.

[10] Long, S., Yao, X., Zhang, X., Delamination prediction in composite laminates under low velocity impact, *Composite Structures,*2015.

[11] Heung Soo Kim, AditiChattopadhyay, AnindyaGhoshal, Characterization of delamination effect on composite

laminates using a new generalized layerwise approach, *Computers and Structures,* Vol. 81, 2003, pp. 1555–1566.
[12] Huang, Y., Liu, J., Huang, X., Zhang, J., Yue, G., Delamination and fatigue crack growth behavior in Fiber Metal Laminates (Glare) under single overloads, *International Journal of Fatigue*, Vol. 78, 2015, pp. 53 –60.
[13] Ebru Dural,FulyaOyar, Effect of delamination size, location and boundary conditions on the behavior of a laminated glass plate, *Structures,* Vol. 47, 2023,pp.121–133.
[14] T.J. de Vries a, A. Vlota, F. Hashagen, Delamination behavior of spliced Fiber Metal Laminates.Part 1. Experimental results, *Composite Structures,*Vol. 46, No. 2, 1999, pp. 131–145.
[15] X. Yongfeng, D. Chen, W. Zhu, G. Li and A. Chattopadhyay, Delamination identification of laminated composite plates using measured mode shapes, *Smart Structures and Systems,*Vol. 23, No. 2, 2019, pp.195–205.
[16] R Sultan, S. Guirguis, M. Younes and E El-Soaly, Delamination detection of composite Laminates using natural frequency Vibration method, *International journal of mechanical engineering and robotics research,*Vol. 1, No. 2, 2012, 286–296.
[17] S.U. Khan, R.C. Alderliesten, R. Benedictus, Delamination growth in Fiber Metal Laminates under variable amplitude Loading, *Composites Science and Technology,* Vol. 69, No.15/16, 2009, pp. 2604–2615.
[18] S. U. Khan, R. C. Alderliesten, R. Benedictus, Delamination in Fiber Metal Laminates (GLARE) during fatigue crack growth under variable amplitude loading, *International Journal of Fatigue,* Vol. 33, No. 9, 2011, pp.1292–1303.
[19] Ganesh Shankar, Jayant Prakash Varuna, P.K. Mahato, Effect of delamination on vibration characteristic of smart laminated composite Plate, *Journal of Aerospace System Engineering,*Vol. 13, No. 4,2019, pp.10–17.
[20] A. Stawiarskia, A. Muca, and, M. Barskia, Experimental and numerical studies of laminated plates with delamination subjected to compressive loads, *Latin American Journal of Solids and Structures,* Vol. 17, No. 5,2020, pp. 1–12.
[21] Kindova-Petrova D. Vibration-based methods for detecting a crack in a simply supported beam. *Journal of Theoretical and Applied Mechanics;* Vol. 44, No. 4,2014, pp. 69–82.
[22] Sultan R, Guirguis S, Younes M, et al. Delamination identification on composite material by free vibration test. *International Journal of Mechanical Engineering and Robotics Research,* Vol. 1, No. 3,2012, pp. 227–236.
[23] Imran M, Khan R and Badshah S. Investigating the effect of delamination size, stacking sequences and boundary conditions on the vibration properties of carbon fiber reinforced polymer composite. *Material Research,* Vol.22, No. 2, 2019, pp. 1-7.
[24] Ren S, Chen G, Li T, et al. A deep learning-based computational algorithm for identifying damage load condition: an artificial intelligence inverse problem solution for failure analysis. *Computer Modeling in Engineering Sciences,* Vol. 117, No. 3,2018, pp. 287–307.
[25] Gope D, Gope PC, Thakur A, Application of artificial neural network for predicting crackgrowth direction in multiple cracks geometry. *Applied soft computing,* Vol. 30, 2015, pp. 514–528.
[26] Elshafey AA, Dawood N, Marzouk H, et al. Crack width in concrete using artificial neural networks. *Engineering Structures,* Vol. 52, 2013, pp. 676–686.
[27] T.G. Srikanth, M. Senthikumar, and S. M. Reddy, Vibration-based delamination evaluation in GFRP composite beam using ANN, *Polymer and polymer composites,* Vol. 29, 2021, pp. 5317 – 5324.
[28] Z. Zhang, K. Shankar, E.V. Morozov, and M. Tahtali, Vibration-based delamination detection in composite beams through frequency changes, *Journal of vibration and control,* Vol. 22, No. 2, 2014, pp. 1– 17.